buildings

MDPI

Article

Study of the Correlation among Luminous Properties of Smart Glazing for Adaptive Energy Saving Buildings

Antonio Piccolo [1,*], Mauro Prestipino [1], Maria Francesca Panzera [2] and Roberto Baccoli [3]

[1] Department of Engineering, University of Messina, Contrada di Dio, 98166 Messina, Italy
[2] Department of Civil, Energy, Environmental and Material Engineering (DICEAM), "Mediterranea" University of Reggio Calabria, Via Graziella, Feo di Vito, 89122 Reggio Calabria, Italy
[3] Department of Civil, Environmental and Architectural Engineering, University of Cagliari, Via Marengo 2, 09123 Cagliari, Italy
* Correspondence: apiccolo@unime.it

Abstract: A smart window, such as electrochromic or thermochromic windows, may not be able to accomplish at the same time energy efficiency and visual comfort functions, since satisfying one criterium interferes with the other. This recalls to the important issue of establishing precise relationships among parameters affecting energy, glare control, and color rendering tasks and the influence on them of glazing material composition and preparation technique. With this aim, the luminous properties of a number of advanced glazings found in literature and of three home-made electrochromic devices differing by material composition and/or preparation technique are analyzed in this study. The investigation has involved the determination of the CIE (Commission International de l'Eclairage) Color Rendering Index (CIE CRI), the Correlated Color Temperature (CCT), and the luminous transmittance coefficient (τ_V) of the devices which are discussed with regard to their potential in absolving to energy and visual comfort tasks. Results lead to the main conclusion that the CIE CRI, CCT, and τ_V indexes are clearly linked by an exponential correlation. At low τ_V values (τ_V < 0.5), however, the correlation weakens and the variation of the CIE CRI and CCT indexes becomes entirely material dependent. The influence of preparation technique appears to be irrelevant since the color rendering indexes appear to be well correlated to τ_V over all the investigated τ_V range.

Keywords: smart windows; color rendition; energy saving; visual comfort

Citation: Piccolo, A.; Prestipino, M.; Panzera, M.F.; Baccoli, R. Study of the Correlation among Luminous Properties of Smart Glazing for Adaptive Energy Saving Buildings. *Buildings* **2023**, *13*, 337. https://doi.org/10.3390/buildings13020337

Academic Editors: Alessandro Cannavale, Marco Pugliese, Fabrizio Mariano and Danny Hin Wa Li

Received: 21 December 2022
Revised: 16 January 2023
Accepted: 19 January 2023
Published: 24 January 2023

1. Introduction

The category of advanced (or smart) windows includes dynamic glazing whose optical properties are capable of reversible changes over the visible and near-infrared spectral region. These devices are essentially multi-pane fenestration components integrating chromogenic coatings and gap-filling materials whose spectral transmittance dynamically changes by effect of a variation in an applied external stimulus. The latter is an electric voltage in the case of electrochromic (EC) windows [1], liquid crystal devices (LCD) [2] and suspended particle devices (SPD) [3], temperature in the case of thermochromic (TC) windows [4], sun irradiance in the case of photochromic (PC) windows [5], and building integrated photovoltaic (BIPV) windows [6] and gas concentration in the case of gasochromic (GC) windows [7]. The remarkable feature of these devices of allowing regulation of the inflow of solar light and heat in buildings, as schematically depicted in Figure 1, enables the accomplishment of specific energy saving requirements (by decreasing energy consumption associated with cooling and lighting) and/or visual comfort tasks (by reducing glare effects from direct/diffuse daylight or cloud brightness). These capabilities assume strategic relevance when considering that the building sector is responsible worldwide for about 40% of the total primary energy consumption and 33% of greenhouse gas emissions [8].

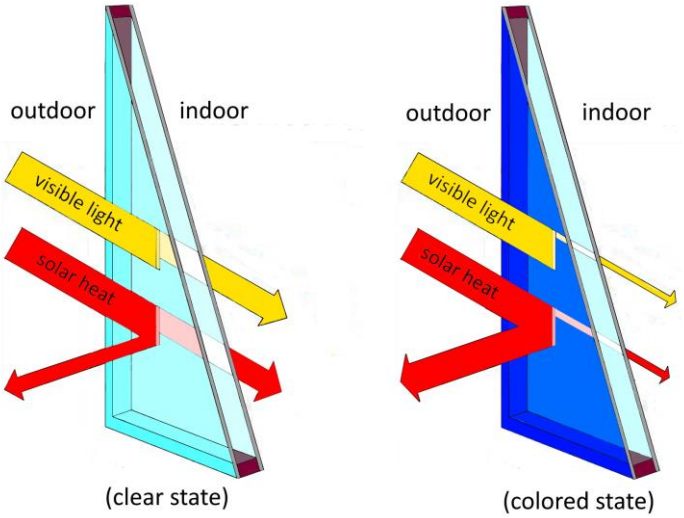

Figure 1. Typical smart windows operating modes.

When analyzing the impact of advanced glazing on the visual quality of indoor environments, however, an important issue to be considered is the color rendition of the transmitted daylight. Indeed, the change in spectral transmittance induces a variation in the spectrum of the incoming radiation (color shift), which significantly affects the perceived color of the illuminated objects. The latter effect deeply influences occupants' behavioral/psychological/health conditions and working performance [9–12].

An important aspect highlighted in many studies [1,13], however, is that smart windows may not be able to fulfil, at the same time, energy efficiency and visual comfort objectives, since satisfying one criterion necessarily interferes with the other. In the case of EC windows, for example, this limitation is evidenced by the circumstance that different control strategies (comfort- or energy-oriented) have considerable diverse impacts on the attainable energy reductions and indoor comfort conditions [14–17]. This recalls, in turn, the critical issue of establishing precise relationships among glazing parameters affecting energy, glare control, and color rendering tasks and the influence of material composition and preparation technique.

Generally, the main parameter considered for assessing the glazing capability in absolving to energy or glare control tasks is the luminous transmittance coefficient τ_V (and related solar transmittance and solar heat gain coefficient) while the main parameters used for estimating the color reproduction properties of the filtered daylight are the traditional CIE (Commission International de l'Eclairage) Color Rendering Index (CIE CRI) and Color Correlated Temperature (CCT) [18], although a number of other indexes can be applied [19].

As a matter of fact, no first direct relation exists among these parameters. Therefore, assessing possible correlations among τ_V, CIE CRI, and CCT and the impact of glazing material composition generally relies on empirical approaches.

Gunde et al. [20] studied the color rendering properties of the light filtered through EC and GC switchable devices. They found for both types of devices that when the luminous transmittance decreases, CIE CRI also decreases and CCT increases. However, the CIE CRI index appears to be not correlated to τ_V, i.e., GC and EC devices characterized by the same τ_V have quite different CIE CRI (except for the bleached and nearly bleached states). The authors found a better correlation between τ_V and CCT, i.e., light filtered by devices having similar τ_V has similar CCT. They concluded that these two indexes likely describe a similar general aspect of daylight, whereas CRI features more spectrally dependent characteristics (color). In both switchable devices, τ_V values below 0.2 correspond to CIE CRI values below 80, the minimum recommended value for appreciable reproduction of colors.

Analogous results were reported by Ghosh and Norton [21] in the case of a home-made WO_3-based EC device and SPD smart glass, respectively. They found that the CCT and CIE CRI indexes increase and decrease respectively at growing coloration levels of the device

and that only for transmittance values above ∼0.1–0.14 the filtered daylight has good color rendition properties (CIE CRI > 80).

A quite different behavior was found by Gosh et al. in polymer-dispersed liquid crystals [2] and dye-sensitized solar cells [22], which exhibited a strong linear correlation between CCT and CIE CRI indexes. In these cases, the higher the CCT the higher the achievable CIE CRI.

No evidence of correlation was found by Liu et al. [6] who analyzed the daylight performance of four cadmium telluride PV windows with different transparencies. Under the 6500 K daylight scenario, it resulted that at increasing values of the luminous transmittance the CCT index first decreases and then increases while the CIE CRI index remains approximately constant.

Roy et al. [23] studied the color rendering performance of three dye-sensitized solar cells differing by TiO_2 thickness. The reduction in luminous transmittance after two years of ambient exposure produced an enhancement of color properties since a favorable increase of CIE CRI and CCT occurred for all devices. The authors concluded that CIE CRI and CCT are not single transmittance dependent values but, rather, spectral dependent parameters.

Dangol et al. [24] analyzed different types of glazing. They concluded that the variation of the CIE CRI and CCT index entirely depends upon the material used to manufacture the window rather than the luminous transmittance coefficient. An analogous conclusion was formulated by Aste et al. [19] who compared the color rendering performance of the main typologies of advanced windows.

The aim of this study is to further investigate the correlation among the τ_V, CIE CRI, and CCT indexes, by also undertaking a preliminary assessment of the influence of preparation technique. To this end, the optical performance in absolving to energy saving, glare control and color rendering tasks of two home-made EC devices prepared by sol-gel process through identical materials but different deposition techniques, namely dip-coating and spin-coating deposition methods, are compared. The influence of manufacturing materials is also analyzed by extending the above investigation to a homemade device previously studied [25] and a number of advanced glazings found in literature including EC, TC, PC, GC, SPD, LCD, and BIPV windows. The results of this work could provide useful information for designers and manufacturers to select proper materials and fabrication processes for the development of smart glazing with enhanced optical properties enabling optimal trade-off between energy saving and visual comfort requirements.

The paper is structured as follows: Section 2 describes the preparation methodology of the three home-made EC devices; Sections 3.1–3.4 deal with the determination of the luminous properties of the devices which are discussed with regard to their potential in absolving to energy and visual comfort tasks; Section 3.5 contains the results and discussion on the correlation among τ_V, CIE CRI, and CCT, while Section 4 focuses on general conclusions.

2. Materials and Methods

Electrochromic devices can be produced by different deposition techniques of films on glass substrates [26]. In general, thin films with thickness ranging from a few nanometers to several micrometers can be deposited using physical techniques, such as vacuum thermal evaporation and sputtering, or chemical techniques, such as sol–gel, chemical vapor deposition, electrodeposition or spry pyrolysis. In the last years, sol–gel deposition has emerged as a cost-effective methodology for preparing EC films for large area-devices. Compared to the other conventional technologies, the sol–gel processing entails a lower manufacturing cost and presents several advantages such as good deposition uniformity over large-area surfaces, use of a great variety of metal oxides and ease of processing (low temperatures and no complex/costly vacuum equipment).

In this work, two EC devices are prepared by the sol–gel process and using the spin-coating and dip-coating deposition methods. Their optical properties are compared to those of a previously investigated device prepared by radio frequency (RF) sputtering [25].

2.1. Sol–Gel: Preparation of Precursor Sol and Film Deposition

The precursor used for the preparation of the sol is acetylated peroxotungstic acid (APTA). To obtain it, 1 g of tungstic acid H_2WO_4 (99%, Sigma Aldrich, St. Louis, MO, USA) was dissolved in 50 mL of an aqueous solution of hydrogen peroxide, H_2O_2 (30%, Sigma Aldrich, St. Louis, MO, USA). The dissolution process was performed at a temperature of 5 °C under continuous stirring for 30 min. Next, the mixture was added with 30 mL of glacial acetic acid (99.7%, Sigma Aldrich, St. Louis, MO, USA) and the solution was heated at 60 °C until it was completely dried. The sol suspension was then prepared by dispersing 250 mg of APTA in 5 mL of absolute ethanol (99.7%, Sigma Aldrich, St. Louis, MO, USA).

This colloidal suspension was deposited on transparent conducting glass substrates coated with indium tin oxide (ITO) (3.7–5.3 Ω/cm^2, Sigma Aldrich, St. Louis, MO, USA) of dimension 5 × 5 cm^2 by both spin-coating and dip-coating deposition techniques under controlled temperature (20 °C) and humidity (40–50%) conditions. In the first case, the spin coater was set to a speed of 2000 rpm; in the second case, the dip-coater was set to a withdrawal speed of 20 cm/min. The resulting films were then heated at 100 °C for 5 min. The whole procedure was repeated three times. Finally, the samples were heated in a muffle from room temperature to 350 °C with a rate of 10 °C/min and then held at this temperature for 3 h.

The switching behavior of the WO_3 films was investigated under lithium ion insertion by using the WO_3-coated ITO-substrates as a working electrode, an ITO-coated glass as a counter electrode, and a solution of CH_3COO:Li as an electrolyte. The samples switched reversibly from a transparent state to a blue color by effect of a low applied potential (±3 V).

2.2. RF Sputtering

The device prepared by RF sputtering has already been investigated in previous studies [25] so only a brief description is given here. The working electrode of the sample, of area 12 × 12 cm^2, comprises a tungsten trioxide (WO_3) layer deposited by RF sputtering from a tungsten trioxide target on glass covered by fluorine-doped tin oxide ("K glass"). The film was deposited for 45 min with a RF sputtering power of 250 W fixing the content of O_2 in the Ar/O_2 gas mixture to 5%. The WO_3 films were then annealed at 908 °C for 1 h. A polymeric electrolyte—poly (ethylene glycol) ethylethermethacrylate (pPEGMA) with lithium dissolved salts—was used as ion conductor while lithium-doped hydrated nickel oxide (NiOH:Li) deposited on K glass formed the "counter-electrode". The device switches reversibly from a transparent state to a blue color by effect of a low applied potential (±2.5 V).

3. Results and Discussion

3.1. Evaluation of the Luminous Transmittance

Figure 2 reports the (near) normal transmittance spectra, measured by a Perkin-Elmer Lamda 9 spectrophotometer in the 300–900 nm wavelength band for the full bleaching and full coloring states of all the investigated devices. Table 1 reports the resulting luminous transmittance values τ_V calculated by the equation [27]:

$$\tau_V = \frac{\sum_{380nm}^{780nm} D_{65}(\lambda)\, V(\lambda)\, \tau(\lambda)\, \Delta\lambda}{\sum_{380nm}^{780nm} D_{65}(\lambda)\, V(\lambda) \Delta\lambda}, \quad (1)$$

where λ is the radiation wavelength, $\tau(\lambda)$ represents the glazing spectral transmittance, $D_{65}(\lambda)$ is the spectral power distribution of illuminant D_{65}, $V(\lambda)$ is the photopic luminous efficiency of the human eye and where $\Delta\lambda$ = 10 nm. In the fourth column of Table 1, the contrast ratio CR of the devices, calculated as the ratio between τ_V in the full bleaching to the full coloring states, is also reported.

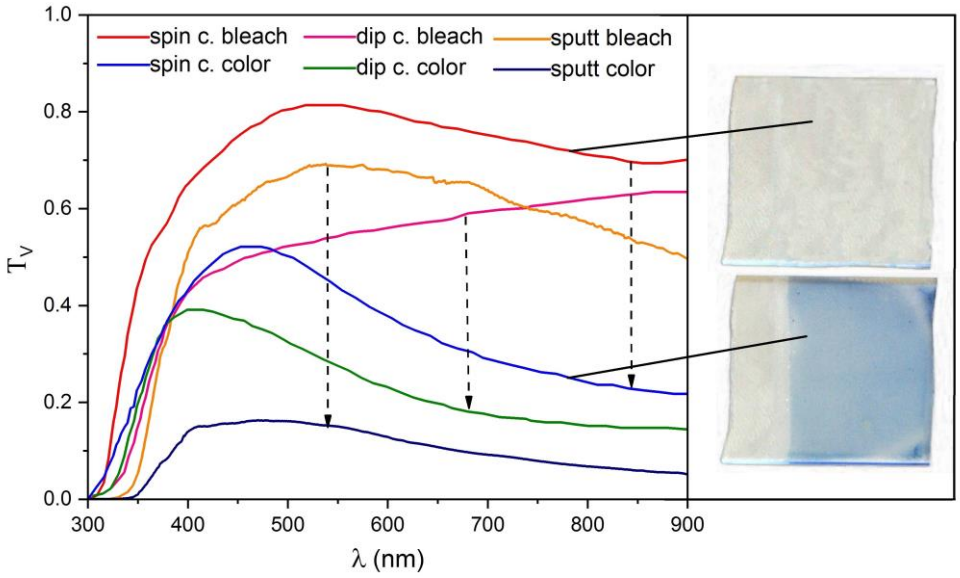

Figure 2. Optical transmittance spectra of the investigated EC devices in the bleached and colored states. A picture of the sample prepared by spin coating in two transmittance states is shown.

Table 1. Calculated parameters. τ_V = luminous transmittance; CR = contrast ratio; (*x*,*y*,*z*) = cromaticity coordinates; CIE CRI = color rendering index, CCT = correlated color temperature.

Device	Switching State	τ_V	CR	*x*	*y*	*z*	CIE CRI	CCT
sol–gel (spin coating)	bleached	0.80	2:1	0.315	0.339	0.346	98.0	6323
sol–gel (spin coating)	colored	0.43		0.283	0.313	0.404	85.4	8719
sol–gel (dip coating)	bleached	0.54	2:1	0.324	0.341	0.335	95.8	5880
sol–gel (dip coating)	colored	0.27		0.272	0.295	0.433	81.6	10,446
sputtering	bleached	0.68	5:1	0.318	0.343	0.338	97.7	6457
sputtering	colored	0.14		0.290	0.324	0.386	85.9	7947

This parameter constitutes an important performance indicator of EC smart windows since it provides a measure of the range of dynamic control (i.e., the transmittance modulation extent) the device can operate. As wide as possible dynamic ranges are desirable to have EC devices able to effectively adapt their optical properties to the time-varying local luminous conditions.

Figure 2 shows how the deposition technique considerably influences the optical properties of the devices. The sample prepared by the sol–gel/dip-coating process exhibits, in fact, a lower visible transmittance compared to the device prepared by spin-coating both in the bleached and in the colored states. Nonetheless, the two samples have comparable contrast ratios (CR≈2:1). On the other hand, the device prepared by sputtering, being based on the complementary electrochromism of WO_3 (the "active" layer) and NiOH:Li (the "ion storage" material), is characterized by a greater dynamic range (CR≈5:1).

Considering the results of relevant case studies [28], it emerges that only the EC sample prepared by RF sputtering, among the investigated devices, possesses specific requisites enabling its use in building applications. Contrast ratios at least equal to 5:1 are deemed acceptable for EC smart glazing in absolving to energy-based tasks (minimization of heating/cooling loads and artificial lighting energy consumption) in different climatic and building scenarios [29]. As an example, a smart window with this dynamic range capability could lead to a total annual energy saving (compared to ordinary glazing) comprised between 6% and 40% for window-to-wall ratios typically equal to 55%, climatic conditions ranging from cooling to heating dominated and when driven by indoor air temperature/global solar radiation/daylight-based control strategies [28]. The devices prepared by sol–gel deposition do not meet these minimum requirements.

The dynamic switching range of the device prepared by sol–gel/dip-coating (0.27–0.54), however, could allow for managing glare effects from diffuse skylight, according to the experimental tests previously conducted by one of the authors [30]. However, none of the above devices can neutralize glare effects from direct sunlight (when the EC glazing is the only operating shade). In this case, in fact, visible transmittances as low as 0.14% are required if the sun is close to the central field of view. The τ_V value increases to 0.6 for non-critical viewing directions [31].

3.2. Evaluation of the Color Coordinates on the CIE-xy 1931 Diagram

The color rendering properties of the light filtered through the investigated EC samples were also studied considering the CIE-*xy* 1931 chromaticity coordinates. To determine them, the tristimulus values for each transmittance spectra reported in Figure 2 have been calculated as:

$$X = \sum_{380nm}^{780nm} D_{65}(\lambda)\ \tau(\lambda)\bar{x}(\lambda)\Delta\lambda \tag{2}$$

$$Y = \sum_{380nm}^{780nm} D_{65}(\lambda)\ \tau(\lambda)\bar{y}(\lambda)\Delta\lambda, \tag{3}$$

$$Z = \sum_{380nm}^{780nm} D_{65}(\lambda)\ \tau(\lambda)\ \bar{z}(\lambda)\Delta\lambda, \tag{4}$$

where ($\bar{x}$,$\bar{y}$,$\bar{z}$) are the color matching functions for the CIE 1931 standard colorimetric observer [27] and $\Delta\lambda$ = 10 nm. The resulting chromaticity coordinates are reported in Table 1 and plotted in Figure 3.

$$x = \frac{X}{X+Y+Z} \quad y = \frac{Y}{X+Y+Z} \quad z = \frac{Z}{X+Y+Z}, \tag{5}$$

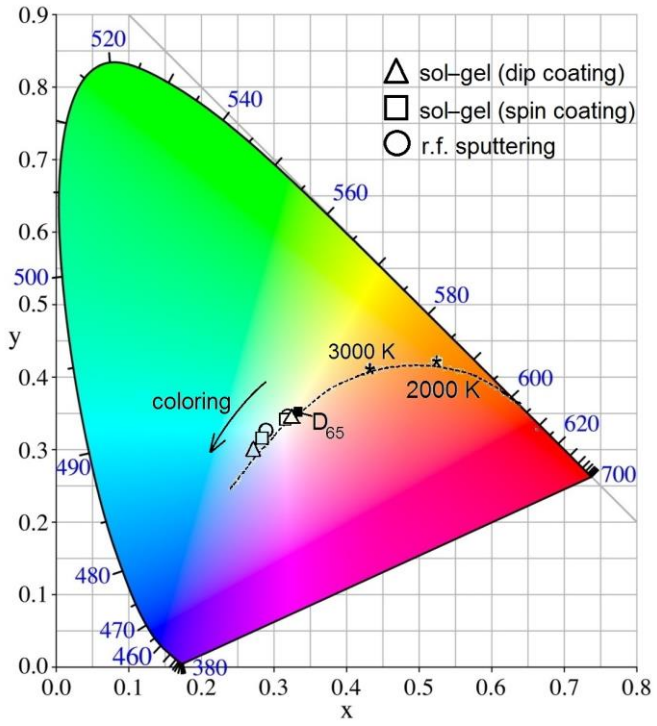

Figure 3. CIE-xy 1931 chromaticity diagram reporting the chromaticity coordinates of the D_{65} light when filtered through the investigated EC glazing switched in the fully bleached and fully colored states. The dashed line represents the blackbody locus with indicated color temperatures (stars). The chromaticity of illuminant D_{65} is represented by the full block.

The graph shows how, for all investigated samples, the chromaticity of the daylight filtered in the clear state is relatively neutral and near the illuminant D_{65} chromaticity (full block). When the devices are switched to the full coloring state, the chromaticity shifts above the blackbody locus in the blue direction, as is typical for WO_3-based EC devices. This is clearly associated with a worsening of the color rendering properties of the light filtered by the devices. The sample prepared by the sol–gel/dip-coating method exhibits the higher color shift, although its transmittance in the full coloring state is higher than that of the device prepared by sputtering. To further investigate this issue, the CIE (Commission International de l'Eclairage) Color Rendering Index (CRI) and Color Correlated Temperature (CCT) are also determined for each transmittance spectrum, as described below.

3.3. Evaluation of the Color Rendering Index CIE CRI

The CIE CRI quantifies the deviation of the color appearance of objects lighted by a test illuminant from the color seen under a reference light source of comparable color temperature. Acceptable illuminants in interiors require a CIE CRI value at minimum equal to 80 (on a maximum of 100). Values higher than 90 are associated to good color perception. The CIE CRI is calculated based on the CIE standard procedure which quantifies the color distortion of eight test-color samples under the reference light source and the light transmitted through the glazing. The first step of the calculation procedure consists in computing the tristimulus values of the light filtered by the glazing and reflected by each test color:

$$X_{t,i} = \sum_{380nm}^{780nm} D_{65}(\lambda)\ \tau(\lambda)\beta_i\ (\lambda)\overline{x}(\lambda)\Delta\lambda \tag{6}$$

$$Y_{t,i} = \sum_{380nm}^{780nm} D_{65}(\lambda)\ \tau(\lambda)\ \beta_i(\lambda)\overline{y}(\lambda)\Delta\lambda, \tag{7}$$

$$Z_{t,i} = \sum_{380nm}^{780nm} D_{65}(\lambda)\ \tau(\lambda)\beta_i(\lambda)\ \overline{y}(\lambda)\Delta\lambda, \tag{8}$$

where $\beta_i(\lambda)$ is the spectral reflectance of each test color (i = 1 to 8).

Then, the total distortion of each color sample (ΔE_i) is obtained by the geometrical distance in the CIE $W^*U^*V^*$ 1964 uniform chromaticity space between the chromatic adaptation transforms (W^*, U^*, V^*) of the eight tests colors when reflecting the light transmitted through the glazing and the direct light of the reference illuminant:

$$\Delta E_i = \sqrt{(U^*_{t,i} - U^*_{r,i})^2 + (V^*_{t,i} - V^*_{r,i})^2 + (W^*_{t,i} - W^*_{r,i})^2}, \tag{9}$$

where subscript "t" refers to the light transmitted through the glazing and subscript "r" refers to the reference illuminant. For the conversion formulas from the CIE-xy 1931 trichromatic components to the CIE $W^*U^*V^*$ 1964 ones the reader is addressed to [27]. The ΔE_i values so obtained allow the calculation of the special color rendering indices R_i for each color sample as

$$R_i = 100 - 4.6\ \Delta E_i, \tag{10}$$

The resulting values are plotted in Figure 4. The general color rendering index CRI is the average of the eight R_i values:

$$\mathrm{CRI} = \frac{1}{8}\sum_{i=1}^{8} R_i, \tag{11}$$

According to the radar plot of the specific R_i index reported in Figure 4, all the investigated EC devices have poor performance in rendering test color 8 (light reddish-purple) when switched to the darkest state ($R_i < 0.8$). The sol–gel/dip-coated device, in addition, exhibits the same inefficiency in rendering test colors 3 (strong yellow green)

and 4 (moderate yellowish green). As for the general CIE CRI index, all devices exhibit values never falling below 80. This suggests that the color appearance of surfaces and objects in a user space equipped with large-scale specimens of these devices should not be subjected to appreciable distortion, even when the EC devices are brought to their highest coloration state. Specifically, the dip-coating device exhibits the lower values of the CIE CRI index in both the fully bleached and fully colored transmitting states, compatibly with the circumstance that its chromaticity coordinates are affected by the largest color shift in the CIE-*xy* 1931 color space. The higher CIE CRI values of the spin coated devices (leading to a more neutral color appearance) are therefore obtained at the expense of a higher visible transmittance both in the clear and dark state. Conversely, the sputtering device has color properties very close to the spin-coated device but, as previously seen, a substantially higher CR (5:1 vs. 2:1).

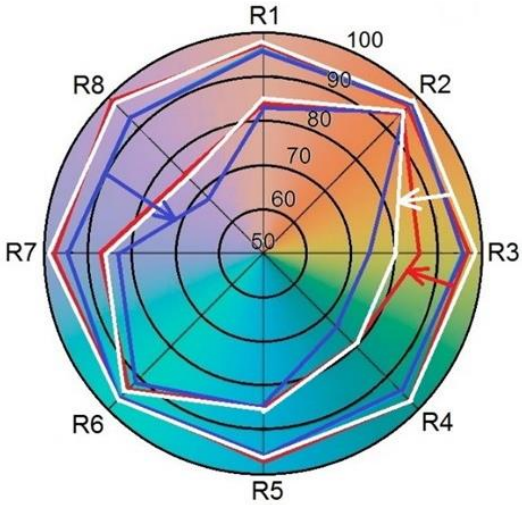

Figure 4. The specific color rendering index R_i of the light filtered through the EC devices for each test color. The blue, white, and red lines refer to the sol–gel/dip-coated, sol–gel/spin-coated, and r.f. sputtered devices, respectively.

3.4. Evaluation of the Correlated Color Temperature CCT

The CCT index accounts for the color appearance of an illuminant and corresponds to the temperature of a Planckian radiator whose chromaticity is closest to the chromaticity of the illuminant. The CCT of natural light varies approximately between 3000 and 1,000,000 K. For indoor spaces, CCT values ranging from 3000 K to 7500 K are generally acceptable [21]. In this work, the CCT index was evaluated with McCamy's equation [32,33].

$$\mathrm{CCT} = -449n^3 + 3525n^2 - 6823.3n + 5520.33 \quad (12)$$

where $n = (x - x_e)/(y - y_e)$, where $x_e = 0.3320$ and $y_e = 0.1858$.

Results reported in Table 1 show how all the investigated EC devices cause in the bleached state a slight reduction of the CCT of the 6500 K (D_{65}) CIE standard light source. Conversely, in all devices, a step increase in the CCT value of the filtered light is registered upon switching to the darkest state. The sample prepared by the sol–gel/dip-coating method causes, in particular, the highest increment, the CCT index growing from 5880 (bleached state) to 10,446 (colored state). This rise could lead to benefits in office spaces where an increase in users' work performance were reported under exposure to blue-enriched white light (CCT = 17,000) [34].

3.5. Study of the Correlation among CRI, CCT, and τ_V

Information on the correlation among CIE CRI, CCT, and τ_V indexes and the associated impact of material composition and preparation technique can be inferred from Figure 5 where the CIE CRI and CCT indexes of the investigated devices and of a number of

advanced glazings found in literature (see the legend of Figure 5) are reported as a function of τ_V. Graph inspection clearly evidences how CIE CRI and τ_V, and likewise CCT and τ_V, are better correlated by exponential rather than by linear regressions. Continuous lines in the upper half diagram (CIE CRI diagram) and lower half diagram (CCT diagram) are least-squares fits of the experimental points by an exponential growth and an exponential decay function, respectively. The coefficients of determination found for the two datasets are R^2 = 0.64 for CIE CRI and R^2 = 0.37 for CCT. This result shows how CCT does not exhibit a stronger correlation with τ_V compared to CIE CRI. This finding does not support therefore the conclusion of Gunde et al. [20], who hypothesized that CCT and τ_V are likely to be well correlated since they should account for a similar general aspect of light while CIE CRI is more "sensible" to its spectral composition.

Based on the obtained regression curves, which represent the average behavior of all the considered smart glazing, it can be observed how at increasing values of the luminous transmittance, the CIE CRI index increases while the CCT index parallelly decreases. Transmittance values below ∼20% seem to be incompatible with good color rendering since the CIE CRI index generally falls below 80, the minimum recommended value for proper reproduction of colors. Transmittance values below ∼30% could lead parallelly to CCT values above 7500 K, the maximum recommended value for indoor environments. These relatively high CCT levels could interfere with visual comfort although they could be accepted by users in office spaces, as discussed in the previous subsection. These circumstances must be considered when evaluating the impact of smart glazing brought to low transmittance levels (for neutralizing, for example, direct glare effects or minimizing radiative heat loads) on the indoor visual quality. In these cases, the integration of additional shading devices, such as overhangs, could be a practical and viable solution [13]. Other strategies for maintaining a neutral spectrum of illumination with EC windows were formulated by Mardaljevic et al. who proposed EC glazing in a combination of clear and full tint panels [35]. Adding Mo to EC WO_3 films also produces an improvement of the color properties since it enhances color neutrality [36].

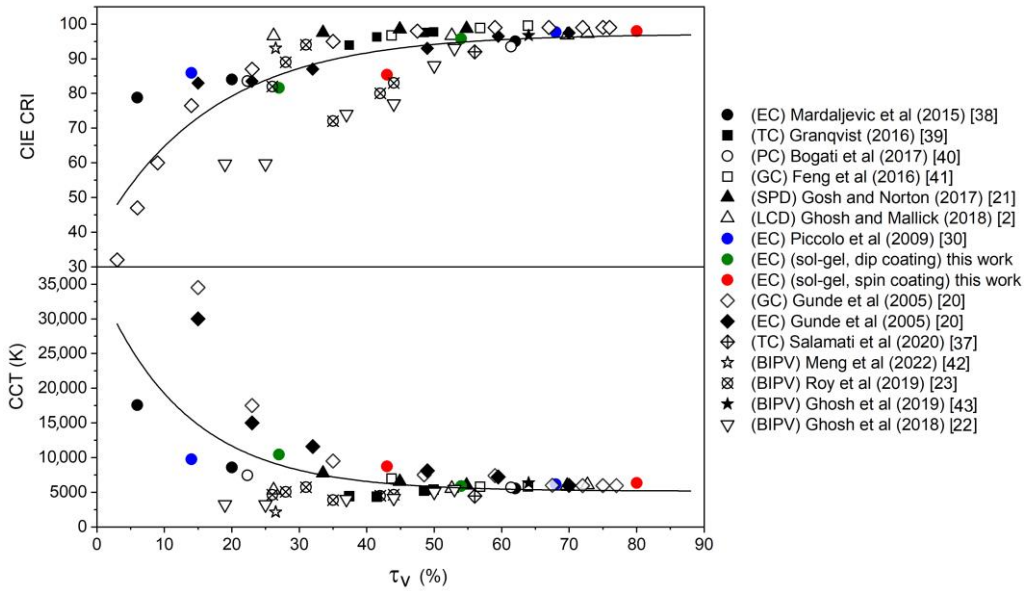

Figure 5. The CIE CRI and CCT indexes as a function of the visible transmittance of selected advanced glazing. Continuous lines are least-squares fits of the experimental points by an exponential growth (upper half diagram) and exponential decay (lower half diagram) function [2,20–23,30,37–43].

As for the influence of material composition on the correlation among CIE CRI, CCT and τ_V the results of this study agree partially with the conclusion of Dangol et al. [24], who evidenced how the increment or decrement of CIE values depends uniquely upon the materials used to manufacture the glazing rather than the luminous transmittance

value. The dispersion of data around the fit curves visible in Figure 5, in fact, reinforces the conclusion of Dangol et al., but limitedly at low τ_V values ($\tau_V < 0.5$). When τ_V increases, a continuous reduction of the dispersion is registered and the points tend to "collapse" on the fitting curves to indicate how the correlation among CIE CRI, CCT, and τ_V becomes stronger and stronger. As expected, the transmittance spectral characteristics of a given material are highly specific at low transmittance values and affect in a peculiar way the color rendering properties of the glazing. However, at high τ_V values spectral composition becomes a less important factor and different glazing/materials behave similarly.

Finally, Figure 5 allows to get some preliminary insight on the influence of preparation technique on the correlation among CIE CRI, CCT, and τ_V as far as the devices prepared by sol–gel synthesis and dip-coating (green full circles) and spin-coating (red full circles) deposition methods are concerned. Although the two devices (made by the same chromogenic materials) exhibit quite different optical properties, the calculated CIE CRI and CCT points fall close to the exponential regression curves. The CIE CRI and CCT indexes, therefore, appear to be well correlated to τ_V over all the investigated τ_V range, so indicating that the influence of preparation technique is not relevant. It must be remarked, however, that this conclusion is based only on the study of two devices and of two deposition techniques (spin-coating vs. dip-coating) and that a wider number of cases should be examined to support it. Therefore, considering this limitation, it may be concluded that material composition, rather than preparation technique, is the main factor determining the variation of the CIE CRI and CCT indexes with τ_V in the low transmittance range ($\tau_V < 0.5$). This requires, for each kind of smart glazing, specific materials engineering research combined with visual comfort analysis addressed at selecting high performing chromogenic substances for optimal trade-off between energy saving and visual comfort [37].

4. Conclusions

In this paper, a study of the correlation among parameters of smart windows affecting energy saving, glare control, and color rendering tasks (i.e., the τ_V, CIE CRI, and CCT indexes) is undertaken. Three home-made EC devices and a number of advanced glazings found in literature differing by material composition and/or preparation technique are investigated.

From the average behavior of all the investigated smart glazing, it can be inferred that at increasing values of the luminous transmittance, the CIE CRI index increases while the CCT index parallelly decreases. Specifically, energy saving or visual control tasks requiring low luminous transmittance values (τ_V < 20–30%), as when the glazing has to minimize the inflow of solar radiation or neutralize direct glare, could interfere with good color reproduction and/or acceptable daylight chromaticity. These low τ_V values are generally associated, in fact, with CIE CRI values below 80 and CCT values above 7500 K. Glare control from diffuse skylight or cloud brightness could be compatible with energy-saving and color-rendering tasks since higher transmittance values are generally involved ($\tau_V > 30\%$).

An exponential correlation among CIE CRI, CCT, and τ_V is clearly visible, but at low τ_V values ($\tau_V < 0.5$), the correlation weakens and the variation of the CIE CRI and CCT indexes becomes entirely material dependent (devices characterized by the same τ_V have quite different CIE CRI and CCT values). The influence of preparation technique on the above correlation appears to be little since the CRI and CCT indexes of devices made by the same chromogenic materials but different preparation techniques appear to be quite well correlated to τ_V over all the investigated τ_V range.

More experimental investigation aimed at exploring a wider number of preparation technologies is however required to support the last conclusion. Future research could also be usefully addressed at studying the influence on the optimal balance between energy saving and visual comfort of climate conditions and users' behavior.

Author Contributions: Conceptualization, A.P.; methodology, A.P.; formal analysis, A.P. and M.P.; investigation, A.P. and R.B.; resources, A.P. and M.P.; data curation A.P., M.P. and R.B.; writing—original draft preparation, A.P. and M.F.P.; writing—review and editing, A.P. and M.F.P.; supervision, A.P., M.P. and R.B. All authors have read and agreed to the published version of the manuscript.

Funding: This research received no external funding.

Data Availability Statement: Not applicable.

Conflicts of Interest: The authors declare no conflict of interest.

Nomenclature

APTA	acetylated peroxotungstic acid
BIPV	building integrated photovltaic
CCT	Correlated Color Temperature (K)
CIE	Commission International de l'Eclairage
CR	contrast ratio
CRI	Color Rendering Index
D_{65}	standard illuminant D_{65}
$D_{65}(\lambda)$	relative spectral power distribution of illuminant D_{65}
EC	electrochromic
GC	gasochromic
ITO	indium tin oxide
K glass	glass covered by fluorine-doped tin oxide
LCD	liquid crystal devices
$n = (x - x_e)/(y - y_e)$,	parameter of McCamy's equation (12)
pPEGMA	poly (ethylene glycol) ethylethermethacrylate
RF	radio frequency
R_i	specific color rendering index of the i-th test color
SPD	suspended particle devices
TC	thermochromic
U^*	chromaticity adaptation transform
$V(\lambda)$	spectral luminous efficiency of the standard observer
V^*	chromaticity adaptation transform
W^*	chromaticity adaptation transform
x	color coordinate on the CIE-xy 1931 chromaticity diagram
$\overline{x}$	CIE standard color matching function
X	CIE tristimulus value
x_e	=0.3320, parameter of McCamy's equation (12)
y	color coordinate on the CIE-xy 1931 chromaticity diagram
$\overline{y}$	CIE standard color matching function
Y	CIE tristimulus value
y_e	=0.1858, parameter of McCamy's equation (12)
z	color coordinate on the CIE-xy 1931 chromaticity diagram
$\overline{z}$	CIE standard color matching function
Z	CIE tristimulus value
Greek symbols	
$\beta_i(\lambda)$	spectral reflectance of i-th test color
ΔE_i	total distortion of i-th test color
$\Delta\lambda$	wavelength interval (nm)
λ	wavelength (nm)
τ	spectral transmittance
τ_V	luminous transmittance coefficient
Subscripts	
i	refers to the i-th test color
r	refers to the reference illuminant
t	refers to light transmitted through glazing
V	luminous, visible

References

1. Cannavale, A.; Ayr, U.; Fiorito, F.; Martellotta, F. Smart electrochromic windows to Enhance Building Energy Efficiency and Visual Comfort. *Energies* **2020**, *13*, 1449. [CrossRef]
2. Ghosh, A.; Mallick, T.K. Evaluation of colour properties due to switching behaviour of a PDLC glazing for adaptive building integration. *Renew. Energy* **2018**, *120*, 126–133. [CrossRef]
3. Nundy, S.; Ghosh, A. Thermal and visual comfort analysis of adaptive vacuum integrated switchable suspended particle device window for temperate climate. *Renew. Energy* **2020**, *159*, 1361–1372. [CrossRef]
4. Aburas, M.; Soebarto, V.; Williamson, T.; Liang, R.; Ebendorff-Heidepriem, H.; Wuc, Y. Thermochromic smart window technologies for building application: A review. *Appl. Energy* **2019**, *255*, 113522. [CrossRef]
5. Wu, L.Y.L.; Zhao, Q.; Huang, H.; Lim, R.J. Sol-gel based photochromic coating for solar responsive smart window. *Surf. Coat. Technol.* **2017**, *320*, 601–607. [CrossRef]
6. Liu, D.; Sun, Y.; Wilson, R.; Wu, Y. Comprehensive evaluation of window-integrated semi-transparent PV for building daylight performance. *Renew. Energy* **2020**, *145*, 1399–1411. [CrossRef]
7. Khaled, K.; Berardi, U. Current and future coating technologies for architectural glazing applications. *Energy Build.* **2021**, *244*, 111022. [CrossRef]
8. Bienvenido-Huertas, D.; Moyano, J.; Marin, D.; Fresco-Contreras, R. Review of in situ methods for assessing the thermal transmittance of walls. *Renew. Sustain. Energy Rev.* **2019**, *102*, 356–371. [CrossRef]
9. Andersen, M.; Gochenour, S.J.; Lockley, S.W. Modelling 'non-visual' effects of daylighting in a residential environment. *Build. Environ.* **2013**, *70*, 138–149. [CrossRef]
10. Bellia, L.; Bisegna, F.; Spada, G. Lighting in indoor environments: Visual and nonvisual effects of light sources with different spectral power distributions. *Build. Environ.* **2011**, *46*, 1984–1992. [CrossRef]
11. Dai, Q.; Cai, W.; Shi, W.; Hao, L.; Wei, M. A proposed lighting-design space: Circadian effect versus visual illuminance. *Build. Environ.* **2017**, *122*, 287–293. [CrossRef]
12. Kim, I.T.; Choi, A.S.; Sung, M.K. Development of a Colour Quality Assessment Tool for indoor luminous environments affecting the circadian rhythm of occupants. *Build. Environ.* **2017**, *126*, 252–265. [CrossRef]
13. Lee, E.S.; Tavil, A. Energy and visual comfort performance of electrochromic windows with overhangs. *Build. Environ.* **2007**, *42*, 2439–2449. [CrossRef]
14. Assimakopoulos, M.N.; Tsangrassoulis, A.; Guarracino, G.; Santamouris, M. Integrated energetic approach for a controllable electrochromic device. *Energy Build.* **2004**, *36*, 415–422. [CrossRef]
15. Assimakopoulos, M.N.; Tsangrassoulis, A.; Santamouris, M.; Guarracino, G. Comparing the energy performance of an electrochromic window under various control strategies. *Build. Environ.* **2007**, *42*, 2829–2834. [CrossRef]
16. Gugliermetti, F.; Bisegna, F. Visual and energy management of electrochromic windows in Mediterranean climate. *Build. Environ.* **2003**, *38*, 479–492. [CrossRef]
17. Cannavale, A.; Ayr, U.; Martellotta, F. Innovative electrochromic devices: Energy savings and visual comfort effects. *Energy Procedia* **2018**, *148*, 900–907. [CrossRef]
18. International Commission on Illumination. *Method of Measuring and Specifying Colour Rendering Properties of Light Sources*; Commission Internationale de l'éclairage; CIE Central Bureau: Vienna, Austria, 1995.
19. Aste, N.; Leonforte, F.; Piccolo, A. Color rendering performance of smart glazings for building applications. *Sol. Energy* **2018**, *176*, 51–61. [CrossRef]
20. Gunde, M.K.; Krasovec, U.O.; Platzer, W.J. Color rendering properties of interior lighting influenced by a switchable window. *J. Opt. Soc. Am.* **2005**, *22*, 416–423. [CrossRef]
21. Ghosh, A.; Norton, B. Interior colour rendering of daylight transmitted through a suspended particle device switchable glazing. *Sol. Energy Mater. Sol. Cells* **2017**, *163*, 218–223. [CrossRef]
22. Ghosh, A.; Selvaraj, P.; Sundaram, S.; Mallick, T.K. The colour rendering index and correlated colour temperature of dye-sensitized solar cell for adaptive glazing application. *Sol. Energy* **2018**, *163*, 537–544. [CrossRef]
23. Roy, A.; Ghosh, A.; Bhandari, S.; Selvaraj, P.; Sundaram, S.; Mallick, T.K. Color Comfort Evaluation of Dye-Sensitized Solar Cell (DSSC) Based Building-Integrated Photovoltaic (BIPV) Glazing after 2 Years of Ambient Exposure. *J. Phys. Chemestry C* **2019**, *123*, 23834–23837. [CrossRef]
24. Dangol, R.; Kruisselbrink, T.; Rosemann, A. Effect of Window Glazing on Colour Quality of Transmitted Daylight. *J. Daylight.* **2017**, *4*, 37–47. [CrossRef]
25. Piccolo, A.; Simone, F. Energy performance of an all solid state electrochromic prototype for smart window applications. *Energy Procedia* **2015**, *78*, 110–115. [CrossRef]
26. Park, S.I.; Quan, Y.J.; Kim, S.H.; Kim, H.; Kim, S.; Chun, D.M.; Lee, C.S.; Taya, M.; Chu, W.S.; Ahn, S.H. A Review on Fabrication Processes for Electrochromic Devices. *Int. J. Precis. Eng. Manuf. Green Technol.* **2016**, *3*, 397–421. [CrossRef]
27. *BS EN 410:1998*; Glass in Building—Determination of Luminous and Solar Characteristics of Glazing. European Committee for Standardization: Brussels, Belgium, 1998.
28. Lantonio, N.A.; Krarti, M. Simultaneous design and control optimization of smart glazed windows. *Appl. Energy* **2022**, *328*, 120239. [CrossRef]
29. Piccolo, A.; Simone, F. Performance requirements for electrochromic smart window. *J. Build. Eng.* **2015**, *3*, 94–103. [CrossRef]

30. Piccolo, A.; Pennisi, A.; Simone, F. Daylighting performance of an electrochromic window in a small scale test-cell. *Sol. Energy* **2009**, *83*, 832–844. [CrossRef]
31. Jain, S.; Karmann, C.; Wienold, J. Behind electrochromic glazing: Assessing user's perception of glare from the sun in a controlled environment. *Energy Build.* **2022**, *256*, 111738. [CrossRef]
32. McCamy, C.S. Correlated color temperature as an explicit function of chromaticity coordinates. *Color Res. Appl.* **1992**, *17*, 142–144. [CrossRef]
33. McCamy, C.S. Correlated color temperature as an explicit function of chromaticity coordinates (Erratum). *Color Res. Appl.* **1993**, *18*, 150.
34. Viola, A.U.; James, L.M.; Schlangen, L.J.M.; Dijk, D.-J. Blue-enriched white light in the workplace improves self-reported alertness, performance and sleep quality. *Scand. J. Work Environ. Health* **2008**, *34*, 297–306. [CrossRef]
35. Mardaljevic, J.; Waskett, R.K.; Painter, B. Neutral daylight illumination with variable transmission glass: Theory and validation. *Light. Res. Technol.* **2016**, *48*, 267–285. [CrossRef]
36. Granqvist, C.G.; Arvizu, M.A.; Qu, H.Y.; Wen, R.T.; Niklasson, G.A. Advances in electrochromic device technology: Multiple roads towards superior durability. *Surf. Coat. Technol.* **2019**, *357*, 619–625. [CrossRef]
37. Salamati, M.; Mathur, P.; Kamyabjou, G.; Taghizade, K. Daylight performance analysis of TiO2@W-VO2 thermochromic smart glazing in office buildings. *Build. Environ.* **2020**, *186*, 107351. [CrossRef]
38. Mardaljevic, J.; Kelly, W.R.; Painter, B. Neutral daylight illumination with electrochromic glazing: Simulation of 'light mixing'. In Proceedings of the 28th Session of the International Commission on Illumination (CIE 2015), Manchester, UK, 28 June–4 July 2015.
39. Granqvist, C.G. Recent progress in thermochromics and electrochromics: A brief survey. *Thin Solid Film.* **2016**, *614*, 90–96. [CrossRef]
40. Bogati, S.; Basnet, R.; Graf, W.; Georg, A. Development of photochromic device with magnetron sputtered titanium dioxide and tungsten trioxide films. *Sol. Energy Mater. Sol. Cells* **2017**, *166*, 204–211. [CrossRef]
41. Feng, W.; Zou, L.; Gao, G.; Wu, G.; Shen, J.; Li, W. Gasochromic smart window: Optical and thermal properties, energy simulation and feasibility analysis. *Sol. Energy Mater. Sol. Cells* **2016**, *144*, 316–323. [CrossRef]
42. Meng, Y.; Tan, Y.; Li, X.; Cai, Y.; Peng, J.; Long, Y. Building-integrated photovoltaic smart window with energy generation and conservation. *Appl. Energy* **2022**, *324*, 119676. [CrossRef]
43. Ghosh, A.; Sundaram, S.; Mallick, T.K. Colour properties and glazing factors evaluation of multicrystalline based semi-transparent Photovoltaic-vacuum glazing for BIPV application. *Renew. Energy* **2019**, *131*, 730–736. [CrossRef]